Peptide-loaded microgels as antimicrobial and anti-inflammatory surface coatings

Lina Nyström [1]; Adam A. Strömstedt [2]; Artur Schmidtchen [3,4]; Martin Malmsten [1,5]**

1. Department of Pharmacy, Uppsala University, P.O. Box 580, SE-751 23 Uppsala, Sweden

2. Pharmacognosy, Department of Medicinal Chemistry, Uppsala University, P.O. Box 574, SE-751 23 Uppsala, Sweden

3. Division of Dermatology and Venereology, Department of Clinical Sciences, Lund University, SE-22184 Lund, Sweden

4. Wound Healing Center, Bispebjerg Hospital, Department of Biomedical Sciences, University of Copenhagen, DK-2100 Copenhagen, Denmark

5. Department of Pharmacy, University of Copenhagen, DK-2100 Copenhagen, Denmark

ABSTRACT: Here we report on covalently immobilized poly(ethyl acrylate-*co*-methacrylic acid) microgels loaded with the host defense peptide KYE28 (KYEITTIHNLFRKLTHRLFRRNFGYTLR), which is derived from human heparin cofactor II, as well as its poly(ethylene glycol)-conjugated (PEGylated) version, KYE28PEG. Peptide loading and release, as well as the consequences of these processes on the microgel and peptide properties, were studied by *in situ* ellipsometry, confocal microscopy, zeta potential measurements, and circular dichroism spectroscopy. The results show that the microgel-peptide interactions are electrostatically dominated, thus promoted at higher microgel charge density, while PEGylation suppresses peptide binding. PEGylation also enhances the α-helix induction observed for KYE28 upon microgel incorporation. Additionally, peptide release is facilitated at physiological salt concentration, particularly so for KYE28PEG, which illustrates the importance of electrostatic interactions. *In vitro* studies on *Escherichia coli* show that the microgel-modified surfaces display potent antifouling properties in both the absence and presence of the incorporated peptide. While contact killing dominates at low ionic strength for the peptide-loaded microgels, released peptides also provide antimicrobial activity in bulk at a high ionic strength. Additionally, KYE28- and KYE28PEG-loaded microgels display anti-inflammatory effects on human monocytes. Taken together, these results not only show that surface-bound microgels offer an interesting approach for local drug delivery of host defense peptides but also illustrate the need to achieve high surface loads of peptides for efficient biological effects.

KEYWORDS: Anti-inflammatory, Antimicrobial peptide, Host defense peptide, Microgel, Surface coating

INTRODUCTION

Biomedical implants and devices play an important role in modern medicine. With the possibility to restore body functions of an aging population, the usage of catheters, artificial heart valves, vascular grafts, and prosthetic joints have dramatically increased during the past decade.[1] Unfortunately, the insertion of a biomaterial always comes with a risk of infection and inflammation, as well as other complications, such as poor tissue integration.[2] Due to the nature of microbial colonization and biofilm formation on implant surfaces, biomaterial-associated infections (BAIs) are not only difficult to treat with systemic antibiotics treatments but often demand secondary revision surgeries. This contributes both to an increased risk for patients and to higher healthcare costs.[2-4] Given the associated risk and costs, and the contrasting demand on material properties, considerable focus has been placed on the development of antimicrobial surface modifications for biomaterials in order to minimize the risk of BAIs and resulting complications.[5, 6] Various strategies have been reported in the literature, which essentially fall into three categories. In the first category, antifouling/bacteria-repelling surfaces seek to prevent protein adsorption and thereby subsequent biofilm formation.[7,8] Alternatively, surfaces can be designed to exhibit contact killing of bacteria, either by designed topography,[9,10] or by tethering antimicrobial agents such as cationic polymers,[11] peptides,[12] enzymes,[13] or nanoparticles[14] that kill adhered bacteria. In a third approach, surfaces are designed to release antibiotics or other antimicrobial agents in order to eradicate both adhered and adjacent planktonic bacteria.[15-17] These different approaches each have their strengths and weaknesses, which are well summarized in a recent review by Cloutier et al.[6] However, biology is inherently complex, and although promising results have been shown in the literature for all of these approaches, there is still a great need for improvement from a biological performance perspective. Consequently, there is increasing interest

in multifunctional coatings that combine the above stated approaches, which ideally provide immune-modulating functions to control inflammation, as well as increased tissue integration and promoted healing.[3, 18]

Microgels are sparsely cross-linked polymeric colloids, displaying pronounced swelling transitions in response to a number of triggers, such as pH, ionic strength, reducing conditions, or specific metabolites. When bound to solid interfaces, various microgels have been found to maintain their intrinsic swelling properties displayed in dispersion, although becoming quantitatively restricted and sometimes nonuniform by the presence of a solid interface.[19] Investigating microgels as biomaterial surface coatings, Bridges et al. reported that poly(NIPAm-*co*-PEG) microgels tethered to poly(ethylene terephthalate) (PET) disks reduced adsorption of fibrinogen and adhesion of primary human monocyte/macrophages *in vitro*.[20] The surface-bound microgels were also shown to reduce leukocyte adhesion and expression of proinflammatory cytokines *in vivo*,[20] as well as to reduce chronic inflammation in a rat model.[21] Similarly, Wang et al. found that sparsely distributed, poly(ethylene glycol-*co*-acrylic acid) surface-bound microgels form an array of adhesive and nonadhesive patches, which promote short-term cell spreading and proliferation of osteoblasts, as well as increase osteoblast motility, and positively influence the cellular processes associated with healing.[22]

Although surface-bound microgels have thus shown some promising results on their own, successful biomaterial performance frequently requires control over several processes, including bacterial infection and inflammation. Local administration of an antimicrobial agent may circumvent the high dosage treatment required due to poor bioavailability at the implant interface, caused by compromised angiogenesis and exacerbated by biofilm matrix proteins and fibrous capsule formation.[23, 24] While conventional antibiotics constitute a natural first choice for

antimicrobial agents incorporated into biomaterials or their surface coatings and have indeed been used for medical devices such as sutures and urinary tract catheters,[1] many biomaterial-associated infections are caused by bacteria resistant to conventional antibiotics. For example, orthopedic implant-associated infection reports include cases of methicillin-resistant *Staphylococcus aureus* (MRSA), vancomycin-resistant *S. aureus* (VRSA), multidrug-resistant *Acinetobacter*, extended spectrum β-lactamase producing enterobacteriaceae (ESBLs), and multidrug-resistant *Pseudomonas aeruginosa.*[25] Therefore, there is an increasing interest in alternatives to conventional antibiotics. One such potential alternative is provided by host defense peptides (HDPs), also frequently referred to as antimicrobial peptides (AMPs). HDPs/AMPs are ≈10-40 residues long amphiphilic peptides with a net positive charge, which may be designed to display potent and broad-spectrum antimicrobial effects that are mainly reached through disrupting the cell membrane of the pathogen. Through this, HDPs/AMPs can also be designed to be potently antimicrobial against bacteria resistant to conventional antibiotics.[26-28] In addition, some AMPs display potent immunomodulatory and anti-inflammatory effects.[29] Although HDP/AMP drug delivery remains relatively sparsely investigated,[30] it can potentially be combined with a number of different types of materials for peptide delivery, including polymeric materials (microgels, multilayers, lattices) and mesoporous silica and related materials. Of these materials, microgels are particularly interesting as they have been previously investigated as drug delivery systems for peptide and biomacromolecule drug delivery,[31] and have been found to provide advantages for therapeutic outcomes, e.g., being able to incorporate considerable amounts of peptides, protecting incorporated peptides from enzymatic degradation,[32] and releasing peptides in response to a number of triggers.[33, 34] However, while factors controlling model peptide loading to, distribution within, and release from microgels have been well studied,[35, 36] few studies have focused on how

these processes relate to the antimicrobial effects of HDP/AMP-loaded microgels, particularly for surface-bound microgels.

In the present investigation, we set out to elucidate key factors determining AMP loading and release to/from surface-bound microgels and, notably, to clarify the relative importance of contact killing and release-mediated effects of these systems *in vitro*. KYE28 (Table 1) was selected as a suitable model peptide. This 28 amino acid long peptide, representing the D helix of human heparin cofactor II (HCII), has previously been shown to possess potent antimicrobial properties against Gram-negative *E. coli* and *P. aeruginosa*, and Gram-positive *S. aureus*, as well as the fungus *Candida albicans*.[37, 38] In addition, KYE28 displays potent anti-inflammatory properties, resulting in suppression of NF-κB, and a range of proinflammatory cytokines *in vitro*. As a result of this, KYE28 was found to significantly enhance the survival rate of mice after challenge by bacterial lipopolysaccharide (LPS).[37] Furthermore, while PEGylation of KYE28 reduces its antimicrobial potency, conditions can still be found where the peptide selectively kills bacteria in blood. In addition, the anti-inflammatory properties of the peptide are only modestly affected by PEGylation, which therefore offers an interesting approach to reduce serum protein binding of the peptide and to increase its half-life in the bloodstream.[38] As microgels, poly(ethyl acrylate-*co*-methacrylic acid) provide a well-defined system suitable for these studies. Such surface-bound microgels were previously investigated *in situ* by quantitative nanomechanical property mapping (QNM) AFM as a function of pH, ionic strength, and microgel charge density.[19] It was found that microgel swelling after surface attachment depend on pH, microgel charge density, and ionic strength in a qualitatively similar manner as the corresponding microgels in suspension. However, surface attachment does induce shape changes in the microgel particles. These experimental results were confirmed by finite element modeling. Furthermore, Nyström et al. showed that the loading

of positively charged poly-L-lysine peptide results in pronounced deswelling of surface-bound microgels[36] For higher Mw peptides, peptide-induced deswelling is lower for surface-bound microgels than for the corresponding microgels in suspension, as a result of surface-induced network deformation and partial peptide exclusion. While providing information regarding the effect of microgel properties during surface attachment and consequences for peptide incorporation, no attempt has been made in previous studies to elucidate the consequences of these effects, in terms of bioactivity, for surface-bound microgels as containers of antimicrobial peptides.

The present investigation therefore aims to clarify factors determining loading and release of AMPs KYE28 and KYE28PEG to surface-bound poly(ethyl acrylate-*co*-methacrylic acid) microgels, using a combination of *in situ* ellipsometry, confocal microscopy, z-potential measurements, and circular dichroism (CD) spectroscopy. The physicochemical information obtained was then correlated to results for the functional performance of these systems regarding antimicrobial and anti-inflammatory effects, both at the interface (‘contact’) and in the solution surrounding the surface-bound microgels (‘release-mediated’).

EXPERIMENTAL SECTION

Materials. Peptides (Table 1) were synthesized by Biopeptide Co., Inc. (San Diego, USA) and were of > 95 % purity (impurities were mainly truncated peptides) as determined by HPLC. All other chemicals were, unless otherwise stated, obtained from Sigma-Aldrich (Schnelldorf, Germany) and were of analytical grade. If not otherwise stated, all experiments were conducted at 20 ºC in 10 mM Tris HCl, pH 7.4, henceforth referred to as Tris buffer.

Table 1. Sequence and key properties of the investigated peptides

Abbreviation	**Sequence**	**M_w** [a] (g/mol)	**IP**[b]	**Z_{net}**[c]
KYE28	KYEITTIHNLFRKLTHRLFRRNFGYTLR	3595	11.86	+6
KYE28PEG	KYEITTIHNLFRKLTHRLFRRNFGYTLR-PEG2200	5851	11.86	+6

a) Molecular weight determined by mass spectrometry. b) Isoelectric point. c) Net charge at pH 7.4.

Microorganisms. *E. coli* ATCC 25922 was obtained from the Department of Clinical Bacteriology at Lund University Hospital, Sweden.

Microgel synthesis and surface preparations. Poly (EA/MAA/BDDA) (ethyl acrylate/ methacrylic acid/ 1,4-butandiol diacrylate) microgels of two different charge densities (66/33/1 or 39/60/1 w/w EA/MAA/BDDA) (~ 100 nm in diameter) were synthesized using seed-feed (starved feed) emulsion polymerization, according to a protocol described elsewhere.[36] Microgels are henceforth abbreviated according to the MAA content in the feed solution: 33 w/w, MAA33; and 60 w/w, MAA60. Control titration of the microgel MAA content yielded 36.9 ± 0.4 w/w % for MAA33 and 63.3 ± 1.5 w/w % for MAA60 (Table S1, Supporting Information). To enable covalent attachment of the MAA-microgels, silica substrates were surface modified with 3-

glycidoxypropyltrimethoxysilane (GOPS) to add epoxy functionality to the interface. The glass substrates, either borosilicate glass coverslips (Fischer Scientific, Västra Frölunda, Sweden), borosilicate glass beads (2 mm in diameter, Sigma-Aldrich, Schnelldorf, Germany) or polished silicon wafers, oxidized to 30 nm thick oxide layer (Semiconductor Wafer Inc., Hsinchu, Taiwan), were cleaned in an acid/base wash before being modified with GOPS, in dried toluene and Hunig´s base (110 °C for 24 h), as described previously.[36] Microgels were deposited by submerging the substrates in a 1 w/w microgel concentration (pH 5.1) in 0.9 mM calcium nitrate, incubated overnight at 50 °C, before unbound microgels were rinsed and the samples were stored in water until further use. The addition of Ca^{2+} ions suppresses the negative effective z-potential of the MAA microgels, from -33 ± 0.3 mV to -23 ± 1.1 mV (Figure S1a, Supporting Information), resulting in substantially higher microgel coverage on the silica substrate (area fractional coverage ≈ 0.45) compared to previously published works (Figure 1a).[19, 36] The increased microgel coverage was shown to increase the peptide-loading capacity of the surface, and the remaining Ca^{2+} ions did not interfere with the electrostatically driven peptide interaction (Figure S1b-c, Supporting Information).

Scanning electron microscopy. Surface-bound MAA microgels were visualized by scanning electron microscopy (SEM). Samples were dried in a desiccator, with alternating vacuum and N_2 (g), prior to visualization by a Zeiss 1530 SEM instrument (Carl Zeiss Microscopy GmbH, Jena, Germany), equipped with an in-lens detector for secondary electrons and operated at a 3.0 kV electron beam accelerating voltage.

Ellipsometry. Peptide adsorption to surface-bound MAA microgels was investigated by null ellipsometry, using an Optrel Multiskop (Optrel, Kleinmachnow, Germany), as described previously.[36, 39] The refractive index increment used for calculating the adsorbed amount was 0.154

cm^3/g, and corrections were routinely made for changes in the bulk refractive index caused by changes in temperature and excess electrolyte concentration. Ellipsometry assumes a layer of uniform composition and a well-defined thickness. Since these conditions were not fulfilled by the presently investigated system (Figure 1A), the adsorbed layer thicknesses are not reported. However, the microgel structure under different conditions was investigated previously by AFM.[19] Prior to the measurements, the substrate was allowed to stabilize in Tris buffer for 30 min before peptide administration. Peptide was added in a stepwise manner (0.5, 1, 5, 10, 25, 50 μM). In each case, peptide binding was monitored until equilibrium, which was a minimum of 30 min before the next addition. Peptide release was then monitored by rinsing in Tris buffer (1 h; 1 mL/min), followed by Tris buffer with additional 150 mM NaCl (1 h; 1 mL/min). Peptide adsorption to GOPS-treated silica substrates without microgels was included as a control. All measurements were made in at least duplicate, and statistical significance between KYE28 and KYE28PEG was established through pooling.

Zeta potential. Microgel effective z-potential with or without incorporated peptides was determined by dynamic light scattering at a 173° scattering angle, using a Zetasizer Nano ZSP (Malvern Instruments, Malvern, U.K.). The electrophoretic mobilities of the microgels (0.01 w/w) were measured in the presence of 10 mM ionic strength and converted to z-potential using the Smoluchowski approximation.[40] Here, it should be noted that the z-potential of diffuse microgel particles is less well-defined than that of solid particles. Hence, the obtained z-potential values should be considered approximate and are therefore referred to as 'effective z-potentials' in the following discussion. Prior to the measurements, the microgels were equilibrated overnight at the indicated peptide concentrations in Tris buffer. Samples were measured in triplicates at 25 °C.

CD spectroscopy. Circular dichroism (CD) spectra were measured by a Jasco J-810 spectropolarimeter (Jasco, Easton, USA) in the range 200-260 nm in Tris buffer. Samples (10 μM peptide, 0.01 w/w microgels) were equilibrated overnight; after which measurements were performed in duplicate at 37 ºC in a 10 mm quartz cuvette under stirring. The α-helix content was calculated from the recorded CD signal at 225 nm, as described previously.[41] Background correction was routinely performed.

Antimicrobial effects. *Bacterial adhesion.* To evaluate bacterial adhesion to surface-bound MAA-microgels, with or without the incorporated peptide, samples was exposed to *E. coli* ATCC 25922. Bacteria were grown to mid-logarithmic phase in 50 mL tryptic soy broth (3 %) at 37 ºC. They were subsequently washed twice by centrifugation and resuspended in buffer (Tris buffer with or without additional 150 mM NaCl) to yield a suspension of 10^8 colony forming units (CFU)/mL, which was verified by absorbance to an optical density of $OD_{600} \approx 0.6$. For peptide loading, microgel-modified glass coverslips (14 mm in diameter) were placed upside down on a drop of 10 μL peptide solution (100 μM) overnight at 5 °C. The peptide-incubated surfaces and controls were then placed face-up in a 24-well plate (15.5 mm inner diameter) before 500 μL of bacteria suspension was added. Next, the surfaces were incubated at 37 °C for 4 h, before they were moved to new wells containing 500 μL Tris buffer in order to remove nonadhered bacteria, and examined by confocal laser scanning microscopy (CLSM). Bacteria were visualized using a 100x/1.25 oil objective on a Confocal Leica DM IRE2 laser scanning microscope (Leica Microsystems, Wetzlar, Germany). The images were collected using Leica TCS SL software (Leica Microsystem, Wetzlar, Germany) and further analyzed using ImageJ Software. Measurements were performed in triplicate at 25 ºC.

Bacteria viability. To investigate the viability of the adhered bacteria, the LIVE/DEAD® Bacterial Viability Kit (*Bac*Light™; Sigma-Aldrich, Schnelldorf, Germany) was used. All bacteria are stained with the green-fluorescent nucleic stain SYTO9, but only cells with impaired membranes are stained red by propidium iodide (PI) nucleic stain.[42] SYTO9 and PI were mixed in a 1:1 ratio, and 1.5 µL was used to stain the 500 µL bacterial solution (15 min, at RT) prior to analysis. The surfaces were removed from solution, placed onto a holder and visualized by CLSM, after which samples were excited with a 488-nm argon laser and emission span of 515-545 nm for SYTO9 and 615-645 nm for PI. Images then further analyzed using ImageJ Software. Measurements were performed in triplicate at 25 ºC.

The viability of planktonic *E. coli* bacteria in the presence of peptide loaded surface-bound MAA microgels was investigated using PrestoBlue® Cell Viability Regent (Thermo Fisher Scientific Inc.). The assay is based on the ability of metabolically active cells to reduce the blue reazurin dye to the pink highly fluorescent resorufin.[43] The samples, either microgel-modified glass coverslips (14 mm in diameter) or glass beads (2 mm in diameter), were prepared as follows. The glass coverslips were prepared in the same manner as for the bacteria adhesion experiment described above. Thereafter, 50 µL of PrestoBlue was added to each well, and samples were further incubated for 30 min (37 ºC) before analysis. The microgel-modified glass beads were incubated in 250 µL Tris buffer or peptide solution overnight in a 24-well plate, after which unbound peptide was rinsed off twice in 1 mL Tris buffer in each well. Excess buffer was then extracted and 300 µL 10^8 CFU/mL *E. coli* in Tris buffer (with or without additional 150 mM NaCl) was added and allowed to incubate for 4 h (37 ºC). Subsequently, 90 µL from each well was transferred to a new 96-well plate and allowed to incubate with an additional 10 µL of PrestoBlue (30 min, 37 ºC) before the fluorescence intensity of each well was measured using a Varioskan Flash Multimode

Reader (Thermo Fisher Scientific, Waltham, USA.), with excitation and emission wavelengths of 560 nm and 590 nm, respectively. Measurements were performed in duplicate at 25 ºC.

NF-κB activation of human monocytes *in vitro*. To investigate the anti-inflammatory properties of peptide-loaded microgels, nonadherent THP1-XBlue-CD14 reporter monocytes (InvivoGen, San Diego, USA), reporting on soluble inflammation inhibitory substances/particles, were cultured according to the manufacturer's instructions. Cells ($1x10^6$ cells/mL) were stimulated with 100 ng/mL *E. coli* (0111:B4) LPS and peptides (incubated with or without 0.001 w/w MAA33-microgels in dispersion) at the indicated concentrations. NF-κB activation was determined after 20 h of incubation according to manufacturer's instructions (InvivoGen, San Diego, USA). Briefly, activation of NF-κB leads to the secretion of embryonic alkaline phosphatase (SEAP) into the cell supernatant. Detection was conducted by mixing the supernatant with a SEAP detection reagent (Quanti-Blue™, InvivoGen, San Diego, USA) followed by absorbance measurement at 600 nm. The data shown were obtained from triplicate measurements.

RESULTS

Peptide-microgel interactions. As the first step in this investigation, peptide incorporation to surface-bound MAA-microgels was investigated by *in situ* ellipsometry (Figure 1b, c). Demonstrating the importance of electrostatics (primarily charge-charge interactions, and entropic effects relating to counterion release) for this process, saturation binding of both KYE28 and KYE28PEG to the anionic surface-bound MAA-microgels was found to be higher for the more highly charged MAA60 microgel than for MAA33 (Figure 1c). PEGylation resulted in a 2-fold reduction of molar absorption for the KYE28 peptide on both microgel variants, implying that the long and bulky PEG-chain hinders peptide diffusion into the polymer network to reach the innermost anionic carboxyl acids. Based on a surface coverage of ~ 0.45 (Figure 1a), the number of peptide molecules bound per MAA33-microgel particle was roughly in the order of magnitude of 24 000 and 10 000 (± 2000) for KYE28 and KYE28PEG, respectively.

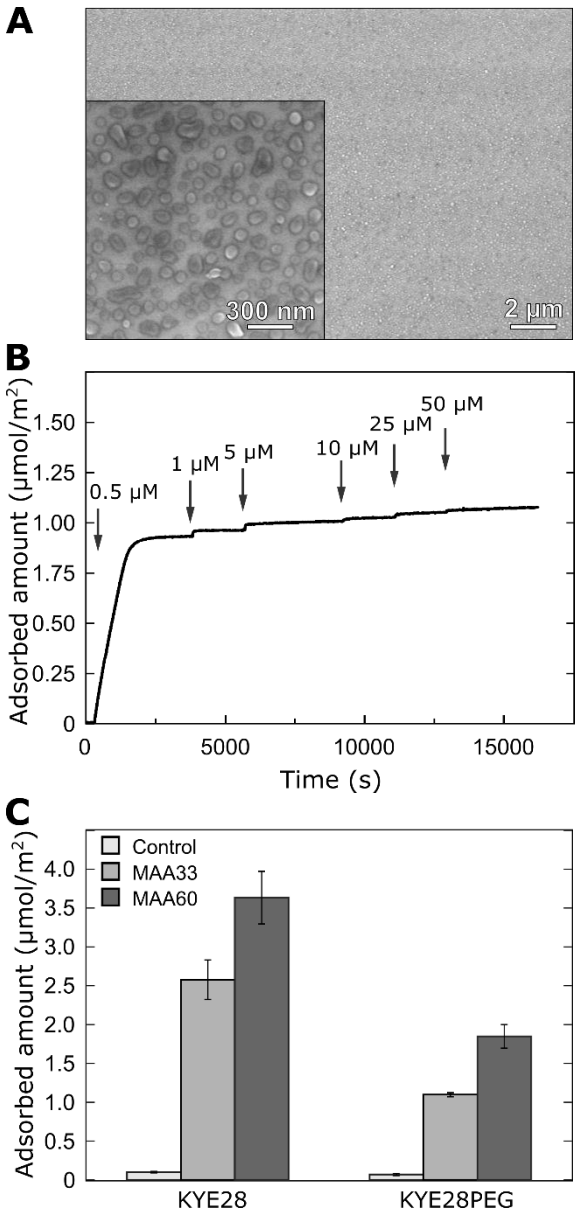

Figure 1. A) Representative SEM images of surface-bound MAA33 microgels. B) Representative kinetic curve of peptide binding to surface-bound MAA33 microgels measured with ellipsometry. KYE28PEG peptide was added in a stepwise manner up to 50 µM in Tris buffer. C) Final adsorption of KYE28 and KYE28PEG (50 µM in Tris buffer) to MAA33 and MAA60 microgels, as well as that of the GOPS-treated control surfaces without microgels.

In dispersion, MAA-microgels have a net negative effective z-potential (≈ -35 mV). With increased loading of oppositely charged peptide, the effective z-potential becomes more negative (Figure 2). However, for KYE28, the loaded microgel particles retain a negative net charge also at a high peptide load, suggesting dilute tails of the anionic microgel network forming the outermost layer of the loaded particles at the highest peptide load investigated. Analogous behavior was previously seen for the AMPs DPK-060 and LL-37[44] at a relatively high microgel concentration. Reducing the microgel concentration at these peptide concentrations was found to allow for complete microgel loading, and hence charge neutralization, for the AMP EFK17.[45] For KYE28PEG, the effective z-potential approaches zero much faster than it does for KYE28, which is in line with the finding of poorer/incomplete penetration of the PEGylated peptide throughout the entire microgel network, suggested by the ellipsometry data. There is little driving force for the water-soluble PEG chains of KYE28PEG to interact with the anionic microgels, making it probable that these peptides are located at the outer periphery of the microgel polymer matrix with a PEG corona surrounding the structure. Analogous effects were observed for MAA60 microgels (Figure S2, Supporting Information).

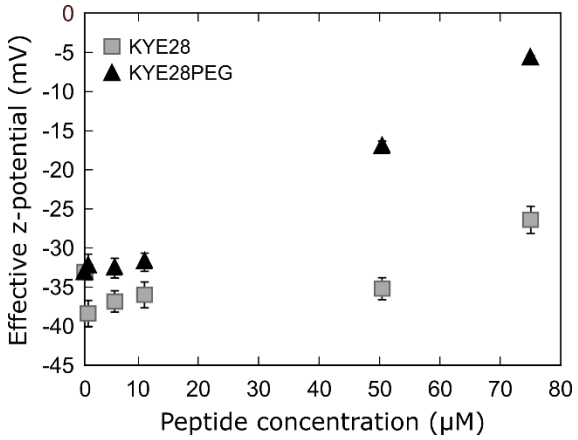

Figure 2. Effective z-potential of dispersed MAA33 microgels (0.01 w/w) in Tris buffer after loading at the indicated peptide concentrations.

To further investigate peptide-microgel interactions, CD measurements were performed to monitor conformational changes of KYE28 and KYE28PEG after microgel incorporation. As shown in Figure 3a and Figure S3, Supporting Information, both peptides undergo conformational changes upon microgel binding, displaying increased α-helical content in the presence of MAA microgels. Quantitatively, helix formation is promoted by higher microgel charge density for KYE28 and by PEGylation, where the latter is probably a consequence of larger conformational freedom in the outer part of the microgels.

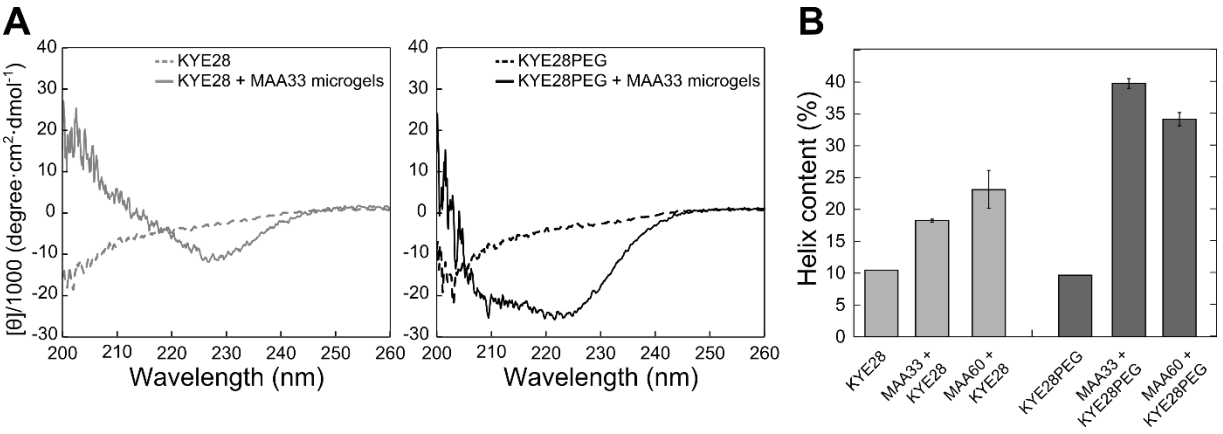

Figure 3. A) CD spectra for KYE28 (left) or KYE28PEG (right) (10 μM in Tris buffer), with or without 0.01 w/w MAA33 microgels. B) Helix content for the indicated peptides in Tris buffer in the presence and absence of 0.01 w/w MAA-microgels.

Peptide release from MAA-microgel layers was subsequently investigated by *in situ* ellipsometry at both low (10 mM) and high (150 mM) ionic strengths. In parallel with the finding that peptide loading increases with microgel charge density, peptide release is quite modest at low ionic strength but promoted at high ionic strength (Figure 4). In particular, KYE28PEG displayed considerable release at high ionic strength, which is in line with the ellipsometry and z-potential data discussed above, indicating that this peptide incorporated primarily in the outer part of the microgel particles.

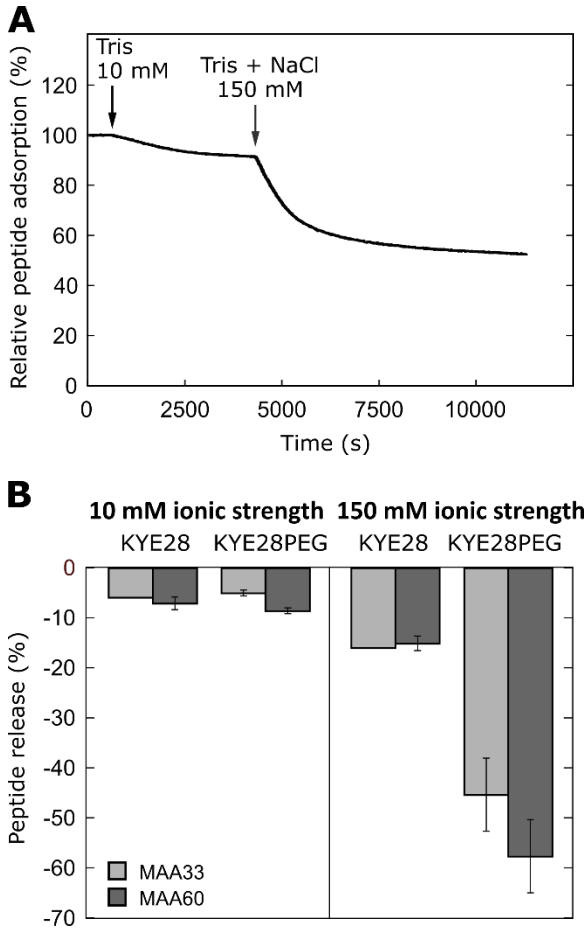

Figure 4. A) Representative kinetic curve obtained by ellipsometry showing the release of KYE28PEG from MAA33 microgels during rinsing with Tris buffer with or without 150 mM NaCl. B) Peptide release from surface-bound MAA-microgels after 1 h of rinsing in a low salt concentration (10 mM Tris), followed by rinsing for 1 h in a high salt concentration (10 mM Tris with additional 150 mM NaCl).

Antimicrobial activity of peptide-loaded surface-bound microgels. To investigate the performance of peptide-loaded surface-bound microgels as antimicrobial coatings, their anti-adhesive properties were assessed next. For this purpose, microgel-coated surfaces were incubated with *E. coli* bacteria, after which nonattached bacteria were gently rinsed off and the remaining attached bacteria were visualized by CLSM. As shown in Figure 5a (top), the untreated (i.e., cleaned, but not microgel-coated) glass displays considerable bacterial adhesion, particularly at the low ionic strength, whereas both the silane-treated (epoxide-containing) and microgel-coated surfaces display low bacterial adhesion, particularly at low ionic strength. After loading with KYE28 and KYE28PEG, bacterial adhesion remains very low at low ionic strength and increases slightly with increasing ionic strength.

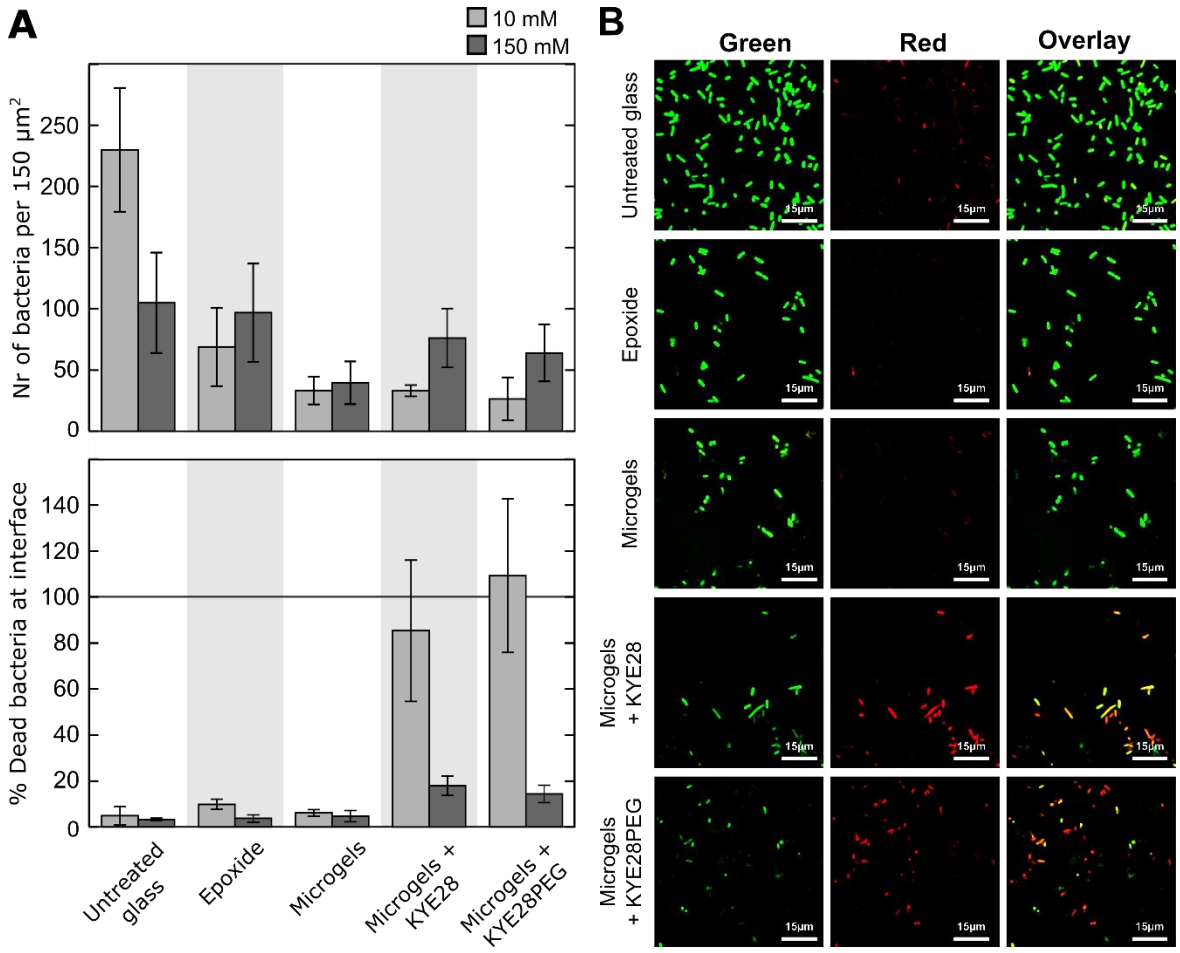

Figure 5. A) Bacterial adhesion of *E. coli* to surface-modified glass slides after 4 h of incubation in Tris buffer with or without additional 150 mM NaCl (top) and viability of the adhered *E. coli* quantified using *Bac*Light® LIVE/DEAD staining (bottom). Data were normalized against *E. coli* killed in 70 % isopropanol. B) Representative CLSM images of adhered *E. coli* on surface-modified glass slides in 10 mM Tris buffer. Images are presented as z-projections of stacks of six images or more, with increased brightness and contrast added after data analyses for improved visualization.

To further investigate the antimicrobial properties of the peptide-loaded microgel coatings, adhered bacteria were stained with LIVE/DEAD staining and viability of the bacteria was analyzed using CLSM imaging. The results show that incorporation of either KYE28 or KYE28PEG (surfaces incubated in 100 μM) results in efficient killing of *E. coli* bacteria (Figures 5a-b). If the surfaces were instead incubated at half the peptide concentration (50 μM), a reduced killing effect was found, as shown in Figure S4. This antimicrobial effect was found to be localized close to the interface (Figure 6a). To demonstrate this localized antimicrobial effect, CLSM images were taken as a z-stack of 8 images at approximately 1 μm apart, vertically from the interface, monitoring red-to-green fluorescence as a function of distance from the microgel surface. At low ionic strength (10 mM), both KYE28 and KYE28PEG were electrostatically bound to the microgel network, with limited/slow peptide release (Figure 6b). Bacterial killing is therefore largely based on direct ('contact') killing. However, at this ionic strength some bacterial killing is also observed at a distance of up to approximately 5 μm from the surface, particularly for KYE28PEG, illustrating the effects of released peptide. The release of dead bacteria is less likely to cause this effect, since bacterial membrane permeabilization by AMPs generally occurs at concentrations much lower than those needed for inducing charge reversal.[46] At physiological 150 mM ionic strength, peptide release is further facilitated, leaving less peptide exposed at the microgel surfaces and in turn resulting in suppressed 'contact' killing effects (Figure 6c). Although, the difference between KYE28 and KYE28PEG did not reach $p < 0.05$. To further demonstrate effects of KYE28 and KYE28PEG released at physiological ionic strength, the viability of planktonic *E. coli* was measured after incubation with peptide-loaded surface-coated microgels. For this, microgels were bound to either modified glass coverslips (14 mm in diameter) as described previously, or glass beads (2 mm in diameter) to increase the area-to-volume ratio. Samples were immersed in bacteria

solution for 4 h (37 ºC) to allow peptide release before the metabolic activity of viable bacteria was monitored by the fluorescent PrestoBlue probe. Although not statistically significant at low ionic strength, the results in Figure 7 suggest that the increase in the surface area-to-volume ratio (and hence the peptide load) offered by the glass beads results in reduced bacterial viability at high ionic strength (i.e., facilitated peptide release). Importantly, these effects were not observed at the low ionic strength (and subsequent low peptide release).

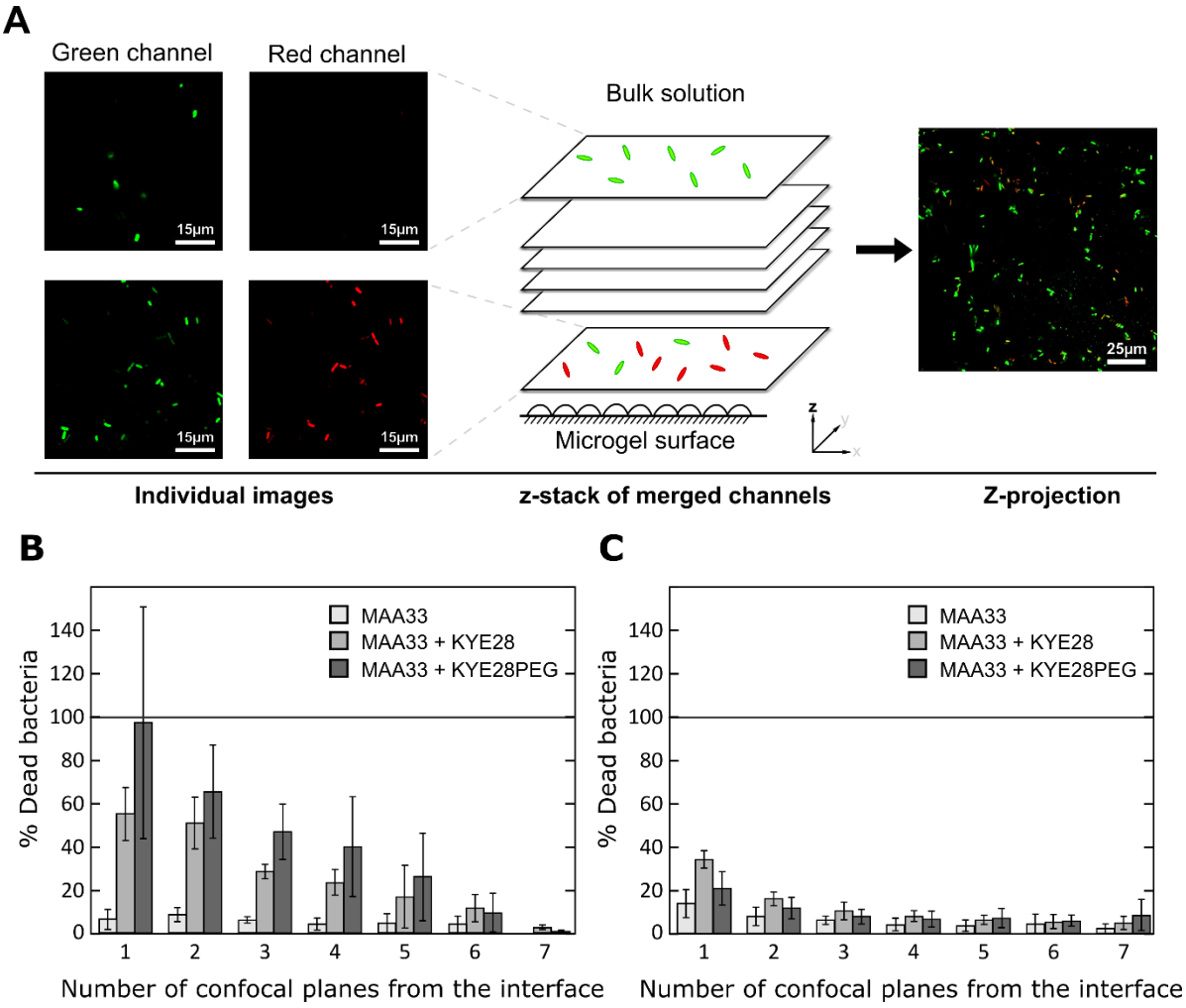

Figure 6. A) Schematic illustration of confocal laser scanning microscopy imaging of the LIVE/DEAD stained adhered *E. coli*. Individual green (SYTO9) and red (PI) channel images were obtained sequentially, at increasing confocal planes, taken vertically in the z-direction from the interface. Channels were subsequently merged and projected into a single image. Representative images in Figure 5B are shown as z-projections of multiple confocal planes. Quantification of the red/green fluorescence intensity ratio of each confocal plane from the interface (interplane distance ≈ 1 µm) was performed in Tris buffer without (B) or with (C) 150 mM NaCl added. Throughout these experiments, the data were normalized to *E. coli* killed in 70 % isopropanol.

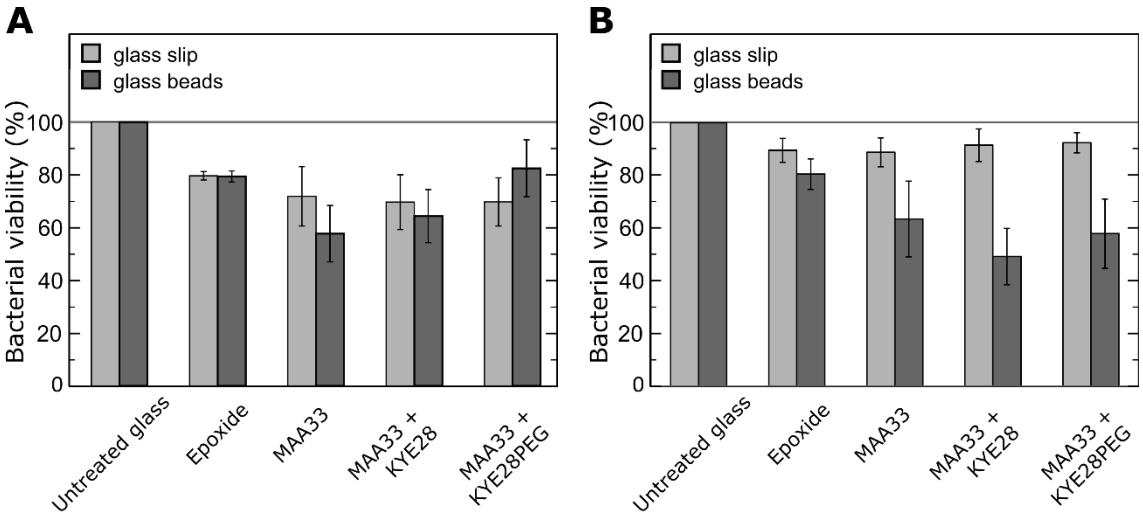

Figure 7. Comparison of planktonic *E. coli* viability in the presence of surface-modified glass slips (14 mm in diameter) and modified glass beads (2 mm in diameter) in Tris buffer, without (A) or with (B) 150 mM NaCl added. The beads increased the surface/volume ratio by 2.7, compared to the slips.

Anti-inflammatory activity of peptide-loaded microgels. In addition to antimicrobial effects, the anti-inflammatory properties of peptide-loaded MAA33 microgels were investigated, as both KYE28 and KYE28PEG have previously been reported to suppress proinflammatory responses.[37, 38] Since LPS-induced cytokine production is dependent on the activation of NF-κB,[47] the anti-inflammatory effects of peptide-loaded MAA33 microgels were investigated for SEAP secretion in human monocytic reporter cells upon stimulation with *E. coli* LPS. The results show that KYE28 and KYE28PEG block LPS-induced NF-κB activation in a dose-dependent manner (Figure 8). Furthermore, MAA33 microgels do not cause any NF-κB activation on their own. Peptide-loaded MAA33 microgels at the concentrations indicated are still able to inhibit NF-κB activation (no statistically significant difference between free and microgel-bound peptides). Cell viability was ensured with MTT assay (Figure S5, Supporting Information).

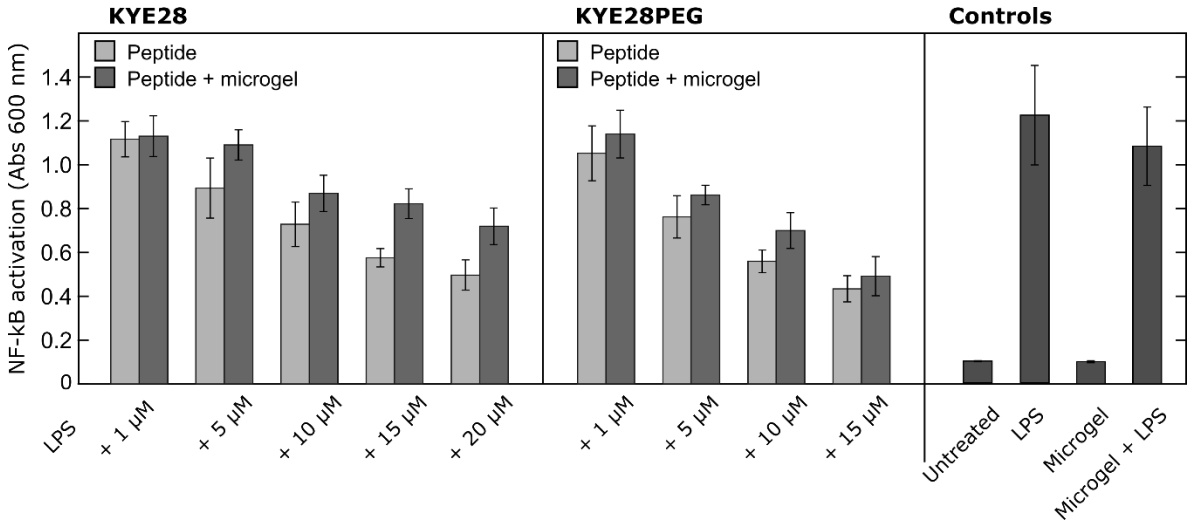

Figure 8. Inhibition of monocyte NF-κB activation by KYE28 and KYE28PEG in the absence and presence of 0.001 w/w MAA33-microgels. THP1-XBlue-CD14 cells were stimulated with 100 ng/mL *E. coli* LPS, and the secretion of embryonic alkaline phosphatase (SEAP) in the cell supernatant (induced by NF-κB) was assessed by absorbance at 600 nm. MAA33 microgels do not activate NF-κB and only slightly interfere with the anti-inflammatory effects of the peptides.

DISCUSSION

Peptide incorporation into and release from microgels has been found to depend on a number of factors. These include microgel charge density and ambient conditions (e.g., pH and ionic strength), as well as various peptide properties, such as charge (distribution), hydrophobicity (distribution), length, and secondary structure.[31] Some of these factors have also been demonstrated to affect the protection of peptides from proteolytic degradation.[32] Conversely, microgel degradation has been reported to be influenced by peptide/protein loading.[48] While there is some information regarding the factors affecting loading and release of model peptides to/from microgels, work on microgel-loaded AMPs remains quite sparse thus far. However, Nordström et al. investigated the incorporation of the antimicrobial peptides LL-37 (LLGDFFRKSKEKIGKEFKRIVQRIKDFLRNLVPRTES) and DPK-060 (GKHKNKGKKNGKHNGWKWWW) in methacrylic acid-based microgels in solution and found that the antimicrobial effects of such systems depended on peptide release, which was promoted for the smaller peptide DPK-060, for low charge density microgels and at a high ionic strength.[44] Furthermore, microgels were demonstrated to protect incorporated AMPs against infection-related proteolysis and to display maintained or improved antimicrobial effects compared to the free peptide, while still displaying modest hemolysis. A similar low toxicity of AMP-loaded microgels was found by Water et al. for novicidin (KNLRRIIRKGIHIIKKYF) in hyaluronic-based microgels.[49] Furthermore, Singh et al. investigated conformational and packing aspects of EFK17 (EFKRIVQRIKDFLRNLV) variants in methacrylic acid-based microgels, and found peptide composition to strongly influence the conformation of microgel-incorporated peptides.[45] Hence, there are a couple studies demonstrating positive functional performance for microgels as delivery systems of AMPs and a couple mechanistic studies, although these focus on microgel dispersions.

In relation to surface-bound hydrogels, a couple of previous studies can be noted, which are primarily related to the biological performance of such systems. Specifically, Zhou et al. investigated methacrylamide hydrogels containing also ε-poly-L-lysine and found these to be antimicrobial against a range of bacteria, yet they displayed modest toxicity against human erythrocytes and keratinocytes.[50] Analogously, Cleophas et al. immobilized inverso-CysHHC10 to PEG hydrogels and found this composite to display good antimicrobial activity to an extent depending on the peptide content.[51] However, in later studies, AMPs were grafted to the hydrogels and the antimicrobial was is achieved only by contact killing. To the best of our knowledge, the relative importance of contact killing and the effects of relying on AMP release for surface-bound microgels loaded with AMPs through physical interactions rather than by covalent coupling has not been previously investigated. In this context, the present study offers new insight in that it demonstrates that peptide release is facilitated for lower charge density microgels and at higher ionic strengths, in analogy to microgels in dispersion. Furthermore, by comparison of microgel dispersions and surface-bound microgels, the present investigation shows that PEGylation precludes peptide incorporation into the microgel interior, which is analogous with the effects of homopolypeptide length and microgel incorporation both in dispersion[52] and at interfaces.[36]

One of the key findings of the present investigation is that contact killing plays a key role in the antimicrobial action of AMP-loaded microgel coatings at a low ionic strength; however, confocal microscopy also demonstrated release-dependent activities. In many ways, these systems are similar to AMP-conjugated hydrogels at these conditions, or to various cationic polymer-based and other surface coatings.[53] On the other hand, at high ionic strength, the AMP-loaded MAA microgels lose much of their contact killing effects as a result of accelerated peptide release, resulting in the distribution of the latter over a much larger volume and hence an effectively lower

peptide concentration. In addition, peptide release is expected to occur from the outside in; hence, fractional release results in decreased AMP exposure at the microgel surface (as seen previously for AMP-loaded mesoporous silica nanoparticles)[54] and reduced antimicrobial effects. Although peptide release should be able to offer some functional advantages compared to surface-grafted AMPs or cationic surface modifications in that killed bacteria are not accumulated at the surface (resulting in transient antimicrobial effects[55]), the present results show that the modest reachable peptide load in dilute monolayer microgel surface coatings, particularly at low surface area-to-bulk volume ratios, precludes released peptide to reach the concentrations required for a potent bactericidal effect. This point to the need to build thicker hydrogel surface coatings, which could be achieved either by polymerizing a hydrogel slab or by bottom-up multilayer constructions of microgel particles, as have been discussed in other contexts.[56, 57] Such studies may also provide further mechanistic insight into how network perturbation induced by the surface propagates throughout the surface-bound microgels. The results obtained previously on this subject is not entirely conclusive. For example, finite element modeling, which captures the effects of pH and microgel charge on microgel deformation, suggests that network deformation is quite local and dissipates within less than 10 % of the microgel volume.[19] In contrast, the results on MAA microgel deswelling, induced by incorporation of positively charged poly-L-lysine of different Mw, demonstrates quantitative differences in peptide-induced deswelling between MAA microgels attached to a surface and those in suspension, suggesting that surface-induced network deformation may indeed propagate to influence the mesh size of the proximal regions of the microgels.[36] In turn, this may have consequences for the properties and functional performance of thicker microgel layers. We are presently in the process of investigating these effects via studies of peptide loading

and release to/from microgel multilayer structures using the same peptides and microgels as in the present study.

Finally, we note that AMP-loaded surface-coatings offer opportunities compared to cationic or other surface coatings that only display direct antimicrobial effects. Specifically, the HDP-loaded microgels also display anti-inflammatory properties, which are important for successful healing and tissue integration of implanted biomaterials.[58] In a related context, Patil et al., investigated PLGA microspheres/PVA hydrogel composites with incorporated vascular endothelial growth factor (VEGF) and dexamethasone *in vivo* in rats and found that this system suppresses inflammation and increases neoangiogenesis of the surrounding tissue.[59] With the potent anti-inflammatory effects displayed by some HDPs, as well as a spectrum of additional biological functionalities,[29] such systems may potentially open the way for surface coatings that display a wider spectrum of biological functionalities for the promotion of biomaterial integration. Indeed, the results of the present investigation demonstrate largely retained anti-inflammatory effects of KYE28 and KYE28PEG after microgel incorporation. However, in regard to the antimicrobial effects of the released peptides, drug load remains a concern with dilute microgel monolayers; hence, microgel-based multilayers may offer more interesting opportunities in this context. Again, promising results for slightly different types of systems indicate that there should be possibilities in this direction.

CONCLUSIONS

In search of multifunctional surface coatings for biomaterials, peptide-loaded, surface-bound, methacrylic acid-based microgels were investigated. Microgel loading of the antimicrobial peptides KYE28 and KYE28PEG was promoted by electrostatic interactions and opposed by steric interactions. The latter was a result of the PEG-conjugation in KYE28PEG, which only partially penetrated the MAA microgels. As a result, peptide release was higher for the PEGylated peptide and was also promoted at high ionic strength. Covalently immobilized MAA-microgels, with or without the incorporated peptide, displayed strong anti-adhesive effect on *E. coli* bacteria. At low ionic strength, bacterial killing by peptide-loaded microgels occurs through both direct contact killing and release of incorporated peptides. On the other hand, at high (physiological) ionic strength, peptide release was facilitated, and the antimicrobial effects were due to the released peptide. As such, the antimicrobial effects depended on the surface area-to-volume ratio, i.e., on the peptide-drug load. Apart from the antimicrobial effects, KYE28 and KYE28PEG loaded on MAA-microgels also displayed anti-inflammatory effects when human monocytes were stimulated with *E. coli* LPS, providing promising results that microgel-based surface coatings loaded with such peptides would result in analogous anti-inflammatory effects if the surface area-to-volume is sufficiently high. Taken together and in relation to previous studies regarding antimicrobial and anti-inflammatory properties of surface-bound microgels as biomaterials surface coatings,[60] the present results offer new insight on factors affecting the interplay between contact killing and release-induced antimicrobial effects of HDP/AMP-loaded surface-bound microgels.

ASSOCIATED CONTENT

Supporting information. Data regarding the effects of calcium ion concentration on microgel surface densities reached, effects on Ca^{2+} on effective microgel z-potential, removability of residual Ca^{2+} by EDTA complexation, CD spectra of KYE28 and KYE28PEG in MAA60 microgels, bacterial adhesion and contact killing, as well as MTT data on cell viability are available as Supporting Information (PDF). This material is available free of charge via the Internet at http://pubs.acs.org.

AUTHOR INFORMATION

Corresponding Authors

* E-mail: lina.nystrom@farmaci.uu.se

* E-mail: martin-malmsten@sund.ku.dk

Notes

The authors declare no competing financial interest.

ACKNOWLEDGMENT

Ann-Charlotte Strömdahl and Sara Malekkhaiat-Häffner are gratefully acknowledged for their skillful technical support. This work was funded by the Swedish Research council (Grant 2016-05157 and 2017-02341) and the LEO Foundation Center for Cutaneous Drug Delivery (project 2016-11-01).

REFERENCES

(1) Riool, M.; de Breij, A.; Drijfhout, J. W.; Nibbering, P. H.; Zaat, S. A. J. Antimicrobial Peptides in Biomedical Device Manufacturing. *Front. Chem.* **2017,** 5, 63.

(2) Darouiche , R. O. Treatment of Infections Associated with Surgical Implants. *N. Engl. J. Med.* **2004,** 350, 1422-1429.

(3) Busscher, H. J.; van der Mei, H. C.; Subbiahdoss, G.; Jutte, P. C.; van den Dungen, J. J. A. M.; Zaat, S. A. J.; Schultz, M. J.; Grainger, D. W. Biomaterial-Associated Infection: Locating the Finish Line in the Race for the Surface. *Sci. Transl. Med.* **2012,** 4, 153rv10-153rv10.

(4) Campoccia, D.; Montanaro, L.; Arciola, C. R. The Significance of Infection Related to Orthopedic Devices and Issues of Antibiotic Resistance. *Biomaterials* **2006,** 27, 2331-2339.

(5) Campoccia, D.; Montanaro, L.; Arciola, C. R. A Review of the Biomaterials Technologies for Infection-Resistant Surfaces. *Biomaterials* **2013,** 34, 8533-8554.

(6) Cloutier, M.; Mantovani, D.; Rosei, F. Antibacterial Coatings: Challenges, Perspectives, and Opportunities. *Trends Biotechnol.* **2015,** 33, 637-652.

(7) Gristina, A. G. Biomaterial-Centered Infection: Microbial Adhesion Versus Tissue Integration. *Science* **1987,** 237, 1588-95.

(8) Yu, Q.; Zhang, Y.; Wang, H.; Brash, J.; Chen, H. Anti-Fouling Bioactive Surfaces. *Acta Biomater.* **2011,** 7, 1550-1557.

(9) Bhadra, C. M.; Khanh Truong, V.; Pham, V. T. H.; Al Kobaisi, M.; Seniutinas, G.; Wang, J. Y.; Juodkazis, S.; Crawford, R. J.; Ivanova, E. P. Antibacterial Titanium Nano-Patterned Arrays Inspired by Dragonfly Wings. *Sci. Rep.* **2015,** 5, 16817.

(10) Diu, T.; Faruqui, N.; Sjöström, T.; Lamarre, B.; Jenkinson, H. F.; Su, B.; Ryadnov, M. G. Cicada-Inspired Cell-Instructive Nanopatterned Arrays. *Sci. Rep.* **2014,** 4, 7122.

(11) Murata, H.; Koepsel, R. R.; Matyjaszewski, K.; Russell, A. J. Permanent, Non-Leaching Antibacterial Surfaces—2: How High Density Cationic Surfaces Kill Bacterial Cells. *Biomaterials* **2007,** 28, 4870-4879.

(12) Humblot, V.; Yala, J.-F.; Thebault, P.; Boukerma, K.; Héquet, A.; Berjeaud, J.-M.; Pradier, C.-M. The Antibacterial Activity of Magainin I Immobilized onto Mixed Thiols Self-Assembled Monolayers. *Biomaterials* **2009,** 30, 3503-3512.

(13) Eby, D. M.; Luckarift, H. R.; Johnson, G. R. Hybrid Antimicrobial Enzyme and Silver Nanoparticle Coatings for Medical Instruments. *ACS Appl. Mater. Interfaces* **2009,** 1, 1553-1560.

(14) Zhao, L.; Wang, H.; Huo, K.; Cui, L.; Zhang, W.; Ni, H.; Zhang, Y.; Wu, Z.; Chu, P. K. Antibacterial Nano-Structured Titania Coating Incorporated with Silver Nanoparticles. *Biomaterials* **2011,** 32, 5706-5716.

(15) Zilberman, M.; Elsner, J. J. Antibiotic-Eluting Medical Devices for Various Applications. *J. Control Release* **2008,** 130, 202-215.

(16) Shukla, A.; Fleming, K. E.; Chuang, H. F.; Chau, T. M.; Loose, C. R.; Stephanopoulos, G. N.; Hammond, P. T. Controlling the Release of Peptide Antimicrobial Agents from Surfaces. *Biomaterials* **2010,** 31, 2348-2357.

(17) Pavlukhina, S.; Lu, Y.-M.; Patimetha, A.; Libera, M.; Sukhishvili, S. Polymer Multilayers with Ph-Triggered Release of Antibacterial Agents. *Biomacromolecules* **2010,** 11, 3448-3456.

(18) Vishwakarma, A.; Bhise, N. S.; Evangelista, M. B.; Rouwkema, J.; Dokmeci, M. R.; Ghaemmaghami, A. M.; Vrana, N. E.; Khademhosseini, A. Engineering Immunomodulatory Biomaterials to Tune the Inflammatory Response. *Trends Biotechnol.* **2016,** 34, 470-482.

(19) Nyström, L.; Álvarez-Asencio, R.; Frenning, G.; Saunders, B. R.; Rutland, M. W.; Malmsten, M. Electrostatic Swelling Transitions in Surface-Bound Microgels. *ACS Appl. Mater. Interfaces* **2016,** 8, 27129-27139.
(20) Bridges, A. W.; Singh, N.; Burns, K. L.; Babensee, J. E.; Lyon, L. A.; Garcia, A. J. Reduced Acute Inflammatory Responses to Microgel Conformal Coatings. *Biomaterials* **2008,** 29, 4605-4615.
(21) Bridges, A. W.; Whitmire, R. E.; Singh, N.; Templeman, K. L.; Babensee, J. E.; Lyon, L. A.; Garcia, A. J. Chronic Inflammatory Responses to Microgel-Based Implant Coatings. *J. Biomed. Mater. Res., Part A* **2010,** 94A, 252-258.
(22) Wang, Q.; Libera, M. Microgel-Modified Surfaces Enhance Short-Term Osteoblast Response. *Colloids Surf., B* **2014,** 118, 202-209.
(23) Glinel, K.; Thebault, P.; Humblot, V.; Pradier, C. M.; Jouenne, T. Antibacterial Surfaces Developed from Bio-Inspired Approaches. *Acta Biomater.* **2012,** 8, 1670-1684.
(24) Harms, A.; Maisonneuve, E.; Gerdes, K. Mechanisms of Bacterial Persistence During Stress and Antibiotic Exposure. *Science* **2016,** 354, aaf4268.
(25) Li, B.; Webster, T. J. Bacteria Antibiotic Resistance: New Challenges and Opportunities for Implant-Associated Orthopedic Infections. *J. Orthop. Res.* **2018,** 36, 22-32.
(26) Zasloff, M. Antimicrobial Peptides of Multicellular Organisms. *Nature* **2002,** 415, 389-395.
(27) Hancock, R. E. W.; Sahl, H.-G. Antimicrobial and Host-Defense Peptides as New Anti-Infective Therapeutic Strategies. *Nat. Biotechnol.* **2006,** 24, 1551-1557.
(28) Pasupuleti, M.; Schmidtchen, A.; Malmsten, M. Antimicrobial Peptides: Key Components of the Innate Immune System. *Crit. Rev. Biotechnol.* **2012,** 32, 143-171.
(29) Hancock, R. E.; Haney, E. F.; Gill, E. E. The Immunology of Host Defence Peptides: Beyond Antimicrobial Activity. *Nat. Rev. Immunol.* **2016,** 16, 321-34.
(30) Nordström, R.; Malmsten, M. Delivery Systems for Antimicrobial Peptides. *Adv. Colloid Interface Sci.* **2017,** 242, 17-34.
(31) Bysell, H.; Mansson, R.; Hansson, P.; Malmsten, M. Microgels and Microcapsules in Peptide and Protein Drug Delivery. *Adv. Drug Delivery Rev.* **2011,** 63, 1172-85.
(32) Månsson, R.; Frenning, G.; Malmsten, M. Factors Affecting Enzymatic Degradation of Microgel-Bound Peptides. *Biomacromolecules* **2013,** 14, 2317-2325.
(33) Bartlett, R. L.; Panitch, A. Thermosensitive Nanoparticles with Ph-Triggered Degradation and Release of Anti-Inflammatory Cell-Penetrating Peptides. *Biomacromolecules* **2012,** 13, 2578-2584.
(34) Nolan, C. M.; Serpe, M. J.; Lyon, L. A. Thermally Modulated Insulin Release from Microgel Thin Films. *Biomacromolecules* **2004,** 5, 1940-1946.
(35) Bysell, H.; Malmsten, M. Visualizing the Interaction between Poly-L-Lysine and Poly(Acrylic Acid) Microgels Using Microscopy Techniques: Effect of Electrostatics and Peptide Size. *Langmuir* **2006,** 22, 5476-5484.
(36) Nyström, L.; Nordström, R.; Bramhill, J.; Saunders, B. R.; Álvarez-Asencio, R.; Rutland, M. W.; Malmsten, M. Factors Affecting Peptide Interactions with Surface-Bound Microgels. *Biomacromolecules* **2016,** 17, 669-678.
(37) Kalle, M.; Papareddy, P.; Kasetty, G.; van der Plas, M. J.; Morgelin, M.; Malmsten, M.; Schmidtchen, A. A Peptide of Heparin Cofactor Ii Inhibits Endotoxin-Mediated Shock and Invasive Pseudomonas Aeruginosa Infection. *PloS one* **2014,** 9, e102577.

(38) Singh, S.; Papareddy, P.; Mörgelin, M.; Schmidtchen, A.; Malmsten, M. Effects of Pegylation on Membrane and Lipopolysaccharide Interactions of Host Defense Peptides. *Biomacromolecules* **2014,** 15, 1337-1345.
(39) De Feijter, J. A.; Benjamins, J.; Veer, F. A. Ellipsometry as a Tool to Study the Adsorption Behavior of Synthetic and Biopolymers at the Air–Water Interface. *Biopolymers* **1978,** 17, 1759-1772.
(40) Pelton, R. Temperature-Sensitive Aqueous Microgels. *Adv. Colloid Interface Sci.* **2000,** 85, 1-33.
(41) Sjögren, H.; Ulvenlund, S. Comparison of the Helix-Coil Transition of a Titrating Polypeptide in Aqueous Solutions and at the Air-Water Interface. *Biophys. Chem.* **2005,** 116, 11-21.
(42) Boulos, L.; Prevost, M.; Barbeau, B.; Coallier, J.; Desjardins, R. Live/Dead Baclight : Application of a New Rapid Staining Method for Direct Enumeration of Viable and Total Bacteria in Drinking Water. *J. Microbiol. Methods* **1999,** 37, 77-86.
(43) O'Brien, J.; Wilson, I.; Orton, T.; Pognan, F. Investigation of the Alamar Blue (Resazurin) Fluorescent Dye for the Assessment of Mammalian Cell Cytotoxicity. *Eur. J. Biochem.* **2000,** 267, 5421-6.
(44) Nordström, R.; Nyström, L.; Andren, O. C. J.; Malkoch, M.; Umerska, A.; Davoudi, M.; Schmidtchen, A.; Malmsten, M. Membrane Interactions of Microgels as Carriers of Antimicrobial Peptides. *J. Colloid Interface Sci.* **2018,** 513, 141-150.
(45) Singh, S.; Datta, A.; Borro, B. C.; Davoudi, M.; Schmidtchen, A.; Bhunia, A.; Malmsten, M. Conformational Aspects of High Content Packing of Antimicrobial Peptides in Polymer Microgels. *ACS Appl. Mater. Interfaces* **2017,** 9, 40094-40106.
(46) Strömstedt, A. A.; Ringstad, L.; Schmidtchen, A.; Malmsten, M. Interaction between Amphiphilic Peptides and Phospholipid Membranes. *Current Opinion in Colloid & Interface Science* **2010,** 15, 467-478.
(47) Takeda, K.; Akira, S. Tlr Signaling Pathways. *Semin. Immunol.* **2004,** 16, 3-9.
(48) Widenbring, R.; Frenning, G.; Malmsten, M. Chain and Pore-Blocking Effects on Matrix Degradation in Protein-Loaded Microgels. *Biomacromolecules* **2014,** 15, 3671-8.
(49) Water, J. J.; Kim, Y.; Maltesen, M. J.; Franzyk, H.; Foged, C.; Nielsen, H. M. Hyaluronic Acid-Based Nanogels Produced by Microfluidics-Facilitated Self-Assembly Improves the Safety Profile of the Cationic Host Defense Peptide Novicidin. *Pharm. Res.* **2015,** 32, 2727-35.
(50) Zhou, C.; Li, P.; Qi, X.; Sharif, A. R. M.; Poon, Y. F.; Cao, Y.; Chang, M. W.; Leong, S. S. J.; Chan-Park, M. B. A Photopolymerized Antimicrobial Hydrogel Coating Derived from Epsilon-Poly-L-Lysine. *Biomaterials* **2011,** 32, 2704-2712.
(51) Cleophas, R. T. C.; Sjollema, J.; Busscher, H. J.; Kruijtzer, J. A. W.; Liskamp, R. M. J. Characterization and Activity of an Immobilized Antimicrobial Peptide Containing Bactericidal Peg-Hydrogel. *Biomacromolecules* **2014,** 15, 3390-3395.
(52) Bysell, H.; Hansson, P.; Malmsten, M. Transport of Poly-L-Lysine into Oppositely Charged Poly(Acrylic Acid) Microgels and Its Effect on Gel Deswelling. *J. Colloid Interface Sci.* **2008,** 323, 60-69.
(53) Malmsten, M. Antimicrobial and Antiviral Hydrogels. *Soft Matter* **2011,** 7, 8725-8736.
(54) Braun, K.; Pochert, A.; Lindén, M.; Davoudi, M.; Schmidtchen, A.; Nordström, R.; Malmsten, M. Membrane Interactions of Mesoporous Silica Nanoparticles as Carriers of Antimicrobial Peptides. *J. Colloid Interface Sci.* **2016,** 475, 161-170.

(55) Yu, Q.; Wu, Z.; Chen, H. Dual-Function Antibacterial Surfaces for Biomedical Applications. *Acta Biomater.* **2015,** 16, 1-13.
(56) Fischer, M.; Vahdatzadeh, M.; Konradi, R.; Friedrichs, J.; Maitz, M. F.; Freudenberg, U.; Werner, C. Multilayer Hydrogel Coatings to Combine Hemocompatibility and Antimicrobial Activity. *Biomaterials* **2015,** 56, 198-205.
(57) Caruso, F.; Trau, D.; Möhwald, H.; Renneberg, R. Enzyme Encapsulation in Layer-by-Layer Engineered Polymer Multilayer Capsules. *Langmuir* **2000,** 16, 1485-1488.
(58) Bridges, A. W.; García, A. J. Anti-Inflammatory Polymeric Coatings for Implantable Biomaterials and Devices. *J. Diabetes Sci. Technol.* **2008,** 2, 984-994.
(59) Patil, S. D.; Papadmitrakopoulos, F.; Burgess, D. J. Concurrent Delivery of Dexamethasone and Vegf for Localized Inflammation Control and Angiogenesis. *J. Controlled Release* **2007,** 117, 68-79.
(60) Nyström, L.; Malmsten, M. Surface-Bound Microgels — from Physicochemical Properties to Biomedical Applications. *Adv. Colloid Interface Sci.* **2016,** 238, 88-104.

TABLE OF CONTENTS GRAPHIC